

# Role of Allyl Group in the Hydroxyl and Peroxyl Radical Scavenging Activity of S-Allylcysteine

Perla D. Maldonado,<sup>\*†</sup> J. Raúl Alvarez-Idaboy,<sup>‡</sup> Adriana Aguilar-González,<sup>†</sup> Alfonso Lira-Rocha,<sup>§</sup> Helgi Jung-Cook,<sup>||</sup> Omar Noel Medina-Campos,<sup>†</sup> José Pedraza-Chaverri,<sup>†</sup> and Annia Galano<sup>\*¶</sup>

<sup>†</sup>Patología Vascular Cerebral, Instituto Nacional de Neurología y Neurocirugía Manuel Velasco Suárez, México DF 14269, Mexico

<sup>‡</sup>Departamento de Física y Química Teórica, Facultad de Química, Universidad Nacional Autónoma de México, México DF 04510, México

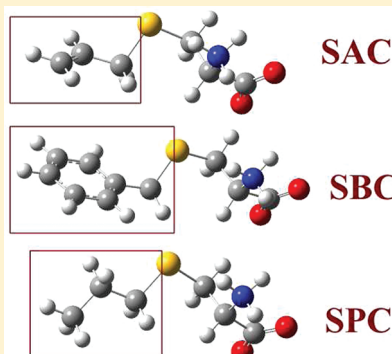
<sup>§</sup>Departamento de Farmacia, Facultad de Química, Universidad Nacional Autónoma de México, México DF 04510, Mexico

<sup>||</sup>Neuropsicofarmacología, Instituto Nacional de Neurología y Neurocirugía Manuel Velasco Suárez, México DF 14269, Mexico

<sup>¶</sup>Departamento de Biología, Facultad de Química, Universidad Nacional Autónoma de México, México DF 04510, Mexico

<sup>\*¶</sup>Departamento de Química, Universidad Autónoma Metropolitana-Iztapalapa, San Rafael Atlixco 186, Col. Vicentina, Iztapalapa, CP 09340, México DF, México

**ABSTRACT:** *S*-Allylcysteine (SAC) is the most abundant compound in aged garlic extracts, and its antioxidant properties have been demonstrated. It is known that SAC is able to scavenge different reactive species including hydroxyl radical ( $\cdot\text{OH}$ ), although its potential ability to scavenge peroxy radical ( $\text{ROO}^{\cdot}$ ) has not been explored. In this work the ability of SAC to scavenge  $\text{ROO}^{\cdot}$  was evaluated, as well as the role of the allyl group ( $-\text{S}-\text{CH}_2-\text{CH}=\text{CH}_2$ ) in its free radical scavenging activity. Two derived compounds of SAC were prepared: *S*-benzylcysteine (SBC) and *S*-propylcysteine (SPC). Their abilities to scavenge  $\cdot\text{OH}$  and  $\text{ROO}^{\cdot}$  were measured. A computational analysis was performed to elucidate the mechanism by which these compounds scavenge  $\cdot\text{OH}$  and  $\text{ROO}^{\cdot}$ . SAC was able to scavenge  $\cdot\text{OH}$  and  $\text{ROO}^{\cdot}$ , in a concentration-dependent way. Such activity was significantly ameliorated when the allyl group was replaced by benzyl or propyl groups. It was shown for the first time that SAC is able to scavenge  $\text{ROO}^{\cdot}$ .



## INTRODUCTION

Aged garlic extracts are odorless products resulting from prolonged extraction of fresh garlic at room temperature; they are highly bioavailable and have biological activity in both animals and humans. The process of aging gently modifies harsh and irritating compounds from raw garlic and naturally generates unique and beneficial compounds through both enzymatic and natural chemical reactions.<sup>1</sup> The main changes in aged garlic extracts during aging processes are the complete hydrolysis of the  $\gamma$ -glutamylcysteines to *S*-allylcysteine (SAC) and *S*-1-propenylcysteine.<sup>2</sup> Numerous data show that aged garlic extracts inhibit the oxidative damage in several experimental models, and this property has been associated with its main components such as SAC.<sup>3</sup>

SAC is a very stable compound: in aged garlic extracts it remains unchanged for up to 2 years.<sup>2</sup> It is a white crystalline powder with a characteristic odor, it has no hygroscopic ability, and its melting point is 223.3–223.7 °C. Stored crystal samples show a slight change into a yellowish color, but no transformation or decomposition is observed. SAC is absorbed in the gastrointestinal tract after oral administration, without any changes.<sup>4</sup> SAC is 30-fold less toxic than other typical garlic compounds, such as allicin and diallyl disulfide.<sup>4,5</sup>

The antioxidant properties of SAC have been reported in several studies. SAC is able to scavenge superoxide anion,<sup>6–8</sup>

hydrogen peroxide,<sup>7–11</sup> hydroxyl radical ( $\cdot\text{OH}$ ),<sup>6,8,12,13</sup> and peroxy nitrite anion.<sup>8,14</sup> In addition, SAC prevents lipid peroxidation<sup>9,13,15–17</sup> and protein oxidation<sup>11</sup> and nitration.<sup>14</sup> Recently, Medina-Campos et al.<sup>8</sup> reported that SAC scavenges hypochlorous acid and singlet oxygen. However, the peroxy radical ( $\text{ROO}^{\cdot}$ ) scavenging activity of SAC has been not evaluated yet.

Numagami et al.<sup>18</sup> demonstrated that compounds presenting a thioallyl group (mainly SAC) exhibited a strong antioxidant capacity in a cerebral ischemia model in rats. They also reported that SAC reduces the infarct volume and brain edema, and prevents peroxy nitrite formation and lipid peroxidation. In this regard, Moriguchi et al.<sup>19</sup> have also reported protective actions from garlic compounds containing a thioallyl group when tested in cerebral atrophy models. SAC not only prevents cerebral atrophy caused by neuronal cell loss in senescence-accelerated mice, but also increases survival and axonal branching from rat hippocampal neurons. Based on these findings, the authors suggested that the thioallyl group is a key factor for neurotrophic activity. Of note, the use of SAC in this model accelerated the axonal branching, thus suggesting that this compound is acting

**Received:** August 25, 2011

**Revised:** October 7, 2011

**Published:** October 13, 2011

not only as an antioxidant agent but also as a neurotrophic molecule. Thus, it has been hypothesized that the thioallyl group in SAC, and other aged garlic extract molecules, is responsible for the antioxidant and neuroprotective effects, as supported by further evidence demonstrating that these agents contribute to reverse the learning and memory deficits observed in two strains of senescent-accelerated mice.<sup>20</sup> Kim et al.<sup>21</sup> found that the presence of the alanyl group and the absence of the oxo group in SAC are essential for the manifestation of neuroprotective activity against ischemic insults and for scavenging  $\cdot\text{OH}$ , suggesting SAC as a potent neuroprotectant. In this work the peroxy radical ( $\text{ROO}^\bullet$ ) scavenging activity of SAC was evaluated, and the effect of the presence or absence of the allyl group on its efficiency for scavenging  $\cdot\text{OH}$  and  $\text{ROO}^\bullet$  was evaluated.

## ■ EXPERIMENTAL METHODS

**Reagents.** L-Cysteine hydrochloride monohydrate, allyl bromide, ascorbic acid, ammonium iron(II) sulfate hexahydrate ( $(\text{NH}_4)_2\text{Fe}(\text{SO}_4)_2 \cdot 6\text{H}_2\text{O}$ ), bovine serum albumin (BSA), Tris·HCl, mercaptoethanol, bromophenol blue, Coomassie brilliant blue, hydrogen peroxide ( $\text{H}_2\text{O}_2$ ), luminol, and 2,2'-azobis(2-methylpropionamidine) dihydrochloride (AAPH) were from Sigma-Aldrich Co. (St. Louis, MO, USA). Absolute ethanol, sodium lumps, benzyl chloride, propyl bromide, trichloroacetic acid, and ethylenediaminetetraacetic acid (EDTA) were from JT Baker (Xalostoc, Edo México, México). In the synthesis of three compounds, all starting materials were commercially available research-grade chemicals and were used without further purification.

**General Information.** Reactions were monitored by analytical thin-layer chromatography on precoated silica gel 60 F<sub>254</sub> plates (Sigma-Aldrich, St. Louis, MO, USA). The solvent system used was 2-propanol– $\text{NH}_4\text{OH}$  (95:5). Spots were visualized with iodine vapors. Melting points were determined on a Fisher-Jones apparatus and are uncorrected. Infrared spectra were recorded on a Nicolet FT-SSX spectrophotometer in KBr pellets. <sup>1</sup>H NMR spectra were recorded on a Varian Unity Inova 400 spectrometer. Deuterium oxide was used as the solvent and internal reference. Chemical shifts are reported in parts per million ( $\delta$ ), and the signals are described as singlet (s), doublet (d), triplet (t), and multiplet (m); coupling constants are reported in hertz. Electron ionization mass spectrometry (EI-MS) was carried out on a JEOL JMS-AX505-HA apparatus. Optical rotation was measured on a Perkin-Elmer Model 241 polarimeter.

**Synthesis of S-Allylcysteine (SAC).** Into a round-bottomed flask, equipped with a mechanical stirrer, was placed L-cysteine hydrochloride monohydrate (30 mmol), and absolute ethanol (90 mL) was added. After 5 min under stirring, 11 mmol of sodium was added in several portions during 30 min to the suspension under vigorous stirring. Next, allyl bromide (31 mmol) was added. After, the mixture was stirred for 1 h, and then cold water (30 mL) was added to obtain a colorless solution. The ethanol was distilled off under reduced pressure and the solution was cooled in an ice bath; acetic acid (2.5 mL) was added (final pH 5.6). The white precipitate was filtered and dried by suction. An analytical sample was obtained by crystallization from absolute ethanol. The same procedure was applied for the preparation of compounds S-benzylcysteine (SBC) and S-propylcysteine (SPC) using the corresponding alkyl halide.

**S-Allylcysteine (SAC).** White solid (70% yield). mp 218–219 °C.  $R_f = 0.71$ . <sup>1</sup>H NMR ( $\text{D}_2\text{O}$ ):  $\delta$  2.94 (dd, 1,  $J = 7.6$ ,

15 Hz,  $\text{H}\beta_1$ ), 3.05 (dd, 1,  $J = 4.4$ , 14.8 Hz,  $\text{H}\beta_2$ ), 3.20 (d, 2,  $J = 7.2$  Hz, –CH<sub>2</sub>-allylic), 3.89 (dd, 1,  $J = 4.4$ , 8.0 Hz, – $\text{H}\alpha$ ), 5.23–5.17 (m, 2, =CH<sub>2</sub>), 5.87–5.77 (m, 1, —CH=). IR (KBr)  $\nu_{\text{max}}$ : 3428 (–NH, str), 2977 (–CH, str), 1616 (–COO–, str), 926 (C–S–C) cm<sup>−1</sup>. EI-MS  $m/z$  (rel int): 161 ( $\text{M}^+$ , 8.18), 116 (9.09), 89 (58.18), 88 (59.9), 87 (100), 74 (77.2), 45 (14.5), 41 (27.2), 39 (10),  $\text{C}_6\text{H}_{11}\text{SO}_2\text{N}$ .  $[\alpha]_D$ : −35.79 (c 1, H<sub>2</sub>O).

**S-Benzylcysteine (SBC).** White solid (60%). mp 215–216 °C.  $R_f = 0.67$ . <sup>1</sup>H NMR ( $\text{D}_2\text{O}$ ):  $\delta$  2.85 (dd, 1,  $J = 4.4$ , 14.6 Hz,  $\text{H}\beta_1$ ), 2.77 (dd, 1,  $J = 7.6$ , 14.8 Hz,  $\text{H}\beta_2$ ), 3.64 (dd, 1,  $J = 4.0$ , 7.6 Hz,  $\text{H}\alpha$ ), 3.66 (s, 2, –S–CH<sub>2</sub>–C<sub>6</sub>H<sub>5</sub>), 7.27–7.181 (m, 5, –C<sub>6</sub>H<sub>5</sub>). IR (KBr)  $\nu_{\text{max}}$ : 3448 (–NH, str), 2945–2616 (–CH, str), 1619 (–COOH, str), 3158–3028 (–CH aryl) 695–767 (–CH aryl, out-of-plane bend) cm<sup>−1</sup>. EI-MS  $m/z$  (rel int): 211 ( $\text{M}^+$ , 2.0), 166 (1.0), 138 (8.0), 134 (9.0), 124 (8.0), 92 (6.0), 74 (5.0), 65 (13), 91 (100),  $\text{C}_{10}\text{H}_{13}\text{SO}_2\text{N}$ .  $[\alpha]_D$ : +25.78 (c 1, H<sub>2</sub>O).

**S-Propylcysteine (SPC).** White solid (70%). mp 205–206 °C.  $R_f = 0.75$ . <sup>1</sup>H NMR ( $\text{D}_2\text{O}$ ):  $\delta$  3.71 (t, 3,  $J = 7.4$  Hz, –CH<sub>3</sub>), 4.37 (sext, 2,  $J = 14.6$  Hz, –CH<sub>2</sub>–), 5.34 (t, 2,  $J = 7.4$  Hz, –S–CH<sub>2</sub>–), 5.87 (dd, 1,  $J = 4.4$ , 14.6 Hz,  $\text{H}\beta_1$ ), 5.77 (dd, 1,  $J = 7.6$ , 14.8 Hz,  $\text{H}\beta_2$ ), 6.71 (dd, 1,  $J = 7.6$  Hz,  $\text{H}\alpha$ ). IR (KBr)  $\nu_{\text{max}}$ : 3429 (–NH), 2871–2961 (–CH), 1580 (–COO–), 1619 (–COO) cm<sup>−1</sup>. EI-MS  $m/z$  (rel int): 163 ( $\text{M}^+$ , 8.0), 161 (2.0), 118 (17.0), 41 (90.0), 74 (37), 61 (41.0), 76 (51.0), 89 (100.0)  $\text{C}_6\text{H}_{13}\text{SO}_2\text{N}$ .  $[\alpha]_D$ : −11.67 (c 1, H<sub>2</sub>O).

**Hydroxyl Radical Scavenging Assay.** Experiments of  $\cdot\text{OH}$ -mediated oxidation of BSA were carried out by using a metal-catalyzed reaction based on Kocha et al.<sup>22</sup> with modifications. A solution of 1.6 mM ascorbic acid/0.8 mM EDTA/0.8 mM ( $\text{NH}_4)_2\text{Fe}(\text{SO}_4)_2$  was prepared in 50 mM phosphate buffer, pH 7.4, and BSA, SAC, SBC, and SPC (0.1–1 mM, final concentrations) were dissolved in it. The assay was made as follows: in 1.5 mL Eppendorf tubes 250  $\mu\text{L}$  of 1% BSA was mixed with 250  $\mu\text{L}$  of the same solution of ascorbic acid/EDTA/( $\text{NH}_4)_2\text{Fe}(\text{SO}_4)_2$  (with SAC, SBC, or SPC). Tubes without SAC, SBC, or SPC were considered as 0% scavenging tubes. The generation of  $\cdot\text{OH}$  was initiated with the addition of 15  $\mu\text{L}$  of 2%  $\text{H}_2\text{O}_2$ . In the control tube (without generation of  $\cdot\text{OH}$ ), the  $\text{H}_2\text{O}_2$  was replaced by water. After 30 min of incubation at room temperature, 250  $\mu\text{L}$  of 20% trichloroacetic acid was added and the mixture was centrifuged at 2236g/30 min/4 °C. The supernatant was discarded and the pellet was resuspended in 500  $\mu\text{L}$  of 0.1 M NaOH. To determine protein damage by  $\cdot\text{OH}$ , the samples were subjected to SDS-PAGE. Forty micrograms of BSA (from resuspended pellet) was mixed 1:1 with loading buffer (10% glycerol, 2% SDS, 25 mM Tris·HCl (pH 6.8), 5% mercaptoethanol, 0.1% bromophenol blue) and heated at 100 °C for 1 min. The protein sample was loaded in a 12.5% polyacrylamide gel and electrophoresed at 100 V. After running, gels were stained with 0.2% Coomassie brilliant blue for 1 h, destained, and scanned in an HP scanner Model 2200c (Hewlett-Packard Co., Palo Alto, CA, USA) for densitometric analysis with SigmaScan Pro software (version 4.01; SPSS Inc., Chicago, IL, USA). The area of each band was obtained and compared to the control band (BSA without SAC, SBC, SPC, or  $\text{H}_2\text{O}_2$ ) and to the 0% scavenging band (BSA with  $\text{H}_2\text{O}_2$  and without SAC, SBC, or SPC).

**Peroxy Radical Scavenging Assay.** Chemiluminescence studies were performed in a Synergy HT Multi Detection microplate reader (Biotek Instruments Inc., Winooski, VT, USA). To evaluate the peroxy radical scavenging activities of SAC, SBC, and SPC, the following experimental procedure was

performed: 25  $\mu\text{L}$  of working solutions of SAC, SBC, and SPC (0.5–2.5 mM, final concentrations) was mixed with 166.67  $\mu\text{L}$  of 30 mM AAPH (generator of peroxy radicals) and 58.3  $\mu\text{L}$  of 21.43  $\mu\text{M}$  luminol in 0.1 M phosphate buffer pH 8.6 in 96-well white microplates (Corning Inc., Lowell, MA, USA), and the luminescence intensity was obtained after 3 min. The luminol stock solution was 50 mM in 2 M NaOH.<sup>23</sup>

Scavenging activity of each compound was expressed as 50% of the inhibitory concentration ( $\text{IC}_{50}$ ) value, which denotes the concentration of the compound required to give a 50% reduction in scavenging capacity relative to the tube without sample. The  $\text{IC}_{50}$  values were calculated by least-squares fitting of plots of concentrations of the compounds versus percent scavenging activity.

**Computational Details.** Geometry optimizations and frequency calculations have been carried out using the M05-2X functional and the 6-311+G(d,p) basis set. The M05-2X functional has been recommended for kinetic calculations by their developers,<sup>24</sup> and it has been also successfully used by independent authors.<sup>25–31</sup> Unrestricted calculations were used for open shell systems, and local minima and transition states were identified by the number of imaginary frequencies (NIMAG = 0 or 1, respectively). Spin contamination was checked for the radical species. In all cases the deviations from the ideal value ( $\langle S^2 \rangle = 0.75$ ) were lower than 2 and 0.05% before and after annihilation of the first spin contaminant. It has been established that for differences within 10% error the obtained results can be trusted.<sup>32,33</sup> Therefore, the spin contamination is negligible for all the radical species studied in this work and their energy values are reliable.

All electronic calculations were performed with the package of programs Gaussian 09.<sup>34</sup> Thermodynamic corrections at 298 K were included in the calculation of relative energies. All the calculations have been performed in aqueous solution, using the continuum density solvation model (SMD).<sup>35</sup> In this model the full solute electron density is used without defining partial atomic charges, and the solvent is represented not explicitly but by a dielectric medium with surface tension at the solute–solvent boundary. SMD is considered to be a universal solvation model, due to its applicability to any charged or uncharged solute in any solvent or liquid medium for which a few key descriptors are known. More details of this model can be found elsewhere.<sup>33</sup>

In all cases the used reference state is 1 M. The solvent cage effects have been included according to the corrections proposed by Okuno,<sup>36</sup> taking into account the free volume theory.<sup>37</sup> These corrections are in good agreement with those independently obtained by Ardura et al.<sup>38</sup> and have been successfully used by other authors.<sup>39–45</sup>

The rate constants ( $k$ ) were calculated using conventional transition state theory (TST)<sup>46–48</sup> and 1 M standard state as

$$k = \sigma \kappa \frac{k_B T}{h} e^{-(\Delta G^\ddagger)/RT} \quad (1)$$

where  $k_B$  and  $h$  are the Boltzmann and Planck constants,  $\Delta G^\ddagger$  is the Gibbs free energy of activation,  $\sigma$  represents the reaction path degeneracy, accounting for the number of equivalent reaction paths, and  $\kappa$  accounts for tunneling corrections. The tunneling corrections defined as the Boltzmann average of the ratio of the quantum and the classical probabilities were calculated using the Eckart barrier.<sup>49</sup>

Some of the calculated rate constants ( $k$ ) values were found to be close to the diffusion-limited rate constant. Accordingly, the

apparent rate constant ( $k_{\text{app}}$ ) cannot be directly obtained from TST calculations. In the present work we have used the Collins–Kimball theory for that purpose.<sup>50</sup>

$$k_{\text{app}} = \frac{k_D k_{\text{act}}}{k_D + k_{\text{act}}} \quad (2)$$

where  $k_{\text{act}}$  is the thermal rate constant, obtained from TST calculations (eq 3), and  $k_D$  is the steady-state Smoluchowski<sup>51</sup> rate constant for an irreversible bimolecular diffusion-controlled reaction:

$$k_D = 4\pi R D_{AB} N_A \quad (3)$$

where  $R$  denotes the reaction distance,  $N_A$  is the Avogadro number, and  $D_{AB}$  is the mutual diffusion coefficient of the reactants A ( $\cdot\text{OH}$  or  $\text{HOO}^\bullet$ ) and B (SAC, SBC, or SPC).  $D_{AB}$  has been calculated from  $D_A$  and  $D_B$  according to ref 52;  $D_A$  and  $D_B$  have been estimated from the Stokes–Einstein approach:<sup>53</sup>

$$D = \frac{k_B T}{6\pi\eta a} \quad (4)$$

where  $k_B$  is the Boltzmann constant;  $T$  is the temperature;  $\eta$  denotes the viscosity of the solvent, in our case water ( $\eta = 8.91 \times 10^{-4}$  Pa s); and  $a$  is the radius of the solute ( $a_{\text{OH}} = 4.79 \text{ \AA}$ ,  $a_{\text{SAC}} = 8.09 \text{ \AA}$ ,  $a_{\text{SBC}} = 8.68 \text{ \AA}$ , and  $a_{\text{SPC}} = 8.13 \text{ \AA}$ ).

**Statistics.** Data are expressed as mean  $\pm$  standard error of the mean (SEM). The scavenging capacity was compared against the tube with 0% scavenging capacity by one way analysis of variance (ANOVA) followed by Dunnett post-test. The  $\text{IC}_{50}$  values were compared by nonpaired *t* test. All data were analyzed using the software Graph Pad 5.01 (San Diego, CA, USA).  $p < 0.05$  was considered as statistically significant.

## ■ RESULTS AND DISCUSSION

**Experimental Results.** SAC was able to scavenge  $\cdot\text{OH}$  (Figure 1A) and  $\text{ROO}^\bullet$  (Figure 1B) in a concentration-dependent way. The efficiency of SBC for scavenging  $\cdot\text{OH}$  was found to be similar to that of SAC (Figure 1A). In contrast, SPC was found to be less effective than SAC for scavenging  $\cdot\text{OH}$  (Figure 1A). The data about the  $\cdot\text{OH}$  scavenging ability of SAC obtained in this study are consistent with the previous results obtained by Medina-Campos et al.<sup>8</sup> In addition, SBC and SPC were found to be less effective than SAC for scavenging  $\text{ROO}^\bullet$  (Figure 1B). The calculated  $\text{IC}_{50}$  of SAC to  $\cdot\text{OH}$  was  $0.27 \pm 0.12$  mM and to  $\text{ROO}^\bullet$  was  $0.7331 \pm 0.567$  mM, which were lower than the values obtained for the other compounds studied, SBC and SPC (Table 1). Thus, these results suggested that SAC reactivity with  $\text{ROO}^\bullet$  is lower compared with  $\cdot\text{OH}$ . This is the first report about the  $\text{ROO}^\bullet$  scavenging ability of SAC.

On the other hand, the  $\cdot\text{OH}$  and  $\text{ROO}^\bullet$  scavenging ability of SAC was significantly ameliorated when the allyl group was changed to a benzyl or propyl group (Figures 1 and 2). These findings indicated that the existence of an allyl group attached to the sulfur atom of the cysteinyl group is necessary for the antioxidant capacity of SAC. Similar results were found by Moriguchi et al.,<sup>19</sup> as SAC significantly and most potently promoted neuronal survival, but S-methyl-, S-ethyl-, and S-propylcysteines were devoid of neurotrophic activity. Furthermore,  $\gamma$ -glutamyl-S-allyl-L-cysteine exerted neurotrophic action in a manner similar to that of SAC while other  $\gamma$ -glutamyl-S-alkyl-L-cysteines having

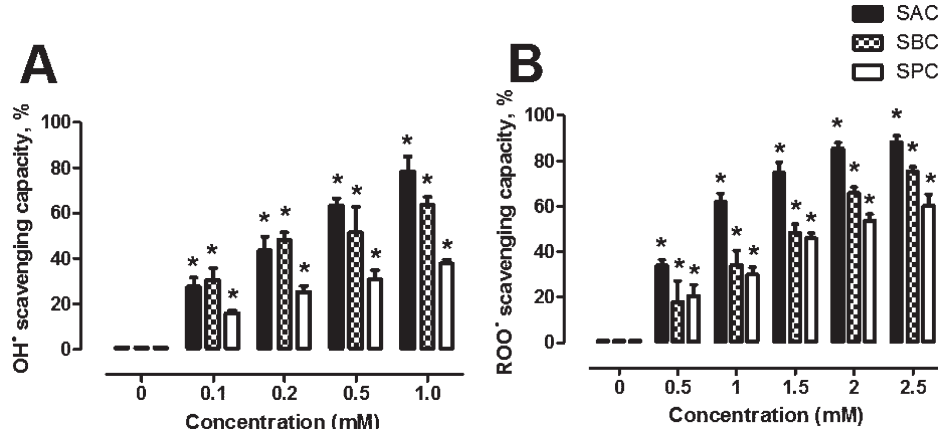


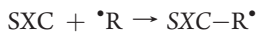
**Figure 1.** Hydroxyl ( $\cdot\text{OH}$ ) (A) and peroxy (ROO $^{\bullet}$ ) (B) radical scavenging capacities of S-allylcysteine (SAC), S-benzylcysteine (SBC), and S-propylcysteine (SPC). Data are mean  $\pm$  SEM.  $n = 3$ . \*  $p < 0.01$  vs 0 mM.

a methyl or propyl group did not support hippocampal neuronal survival.

**Computational Modeling.** Two different structures of SAC, SBC, and SPC have been modeled: the canonical and the zwitterionic forms. It was found that the latter is 6.69, 4.52, and 5.25 kcal/mol lower in Gibbs free energy than the canonical one for SAC, SBC, and SPC, respectively. This indicates that the zwitterionic form will prevail in aqueous solution. It also indicates that it is necessary to perform geometry optimizations in solution to properly reproduce the experimental behavior.

The zwitterionic structures, as well as the site numbers assigned to each reaction site in this work, are shown in Figure 2. The antioxidant activity of the studied compounds has been modeled using the reactions with  $\cdot\text{OH}$  and HOO $^{\bullet}$ . The latter was chosen to represent the ROO $^{\bullet}$  family because of its simplicity. The comparative study of the reactivities of the three antioxidants (SXC, with X = A, B, or P) has been performed for their reactions with  $\cdot\text{OH}$ . All the studied reactions can proceed through different mechanisms. Those considered in the present work are the following:

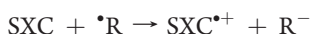
radical adduct formation (RAF):



hydrogen atom transfer (HAT):



single electron transfer (SET):



However, SET can occur not only alone but rapidly followed by, or simultaneously with, proton transfer. These processes are known as sequential electron proton transfer (SEPT) and proton coupled electron transfer (PCET), respectively. Such processes have been also taken into account.

The Gibbs free energies of reaction ( $\Delta G$ ), at room temperature, are reported in Table 2. The SET mechanism was found to be significantly endergonic in all the studied cases. Since the corresponding  $\Delta G$  values are much larger than any inaccuracy of the used methodology, SET has been ruled out for the scavenging activity of SAC, SBC, and SPC when reacting with  $\cdot\text{OH}$ , and

**Table 1.** Scavenging Activity of Hydroxyl ( $\cdot\text{OH}$ ) and Peroxyl (ROO $^{\bullet}$ ) Radicals of SAC, SBC, and SPC (IC<sub>50</sub> Values)<sup>a</sup>

compound	IC <sub>50</sub> values (mM)	
	$\cdot\text{OH}$	ROO $^{\bullet}$
SAC	0.27 $\pm$ 0.12	0.73 $\pm$ 0.05
SBC	0.35 $\pm$ 0.19 <sup>b</sup>	1.45 $\pm$ 0.16 <sup>b</sup>
SPC	ND	1.69 $\pm$ 0.05 <sup>b</sup>

<sup>a</sup> Data are mean  $\pm$  SEM. The number of independent assays was three. SAC, S-allylcysteine; SBC, S-benzylcysteine; SPC, S-propylcysteine; ND, not determined. <sup>b</sup>  $p < 0.05$  vs SAC value.

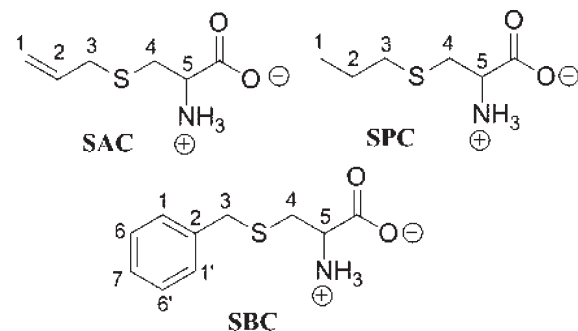


**Figure 2.** Structures and site numbers for S-allylcysteine (SAC), S-benzylcysteine (SBC), and S-propylcysteine (SPC).

also for SAC when reacting with HOO $^{\bullet}$ . Since SET is the first step of the SEPT mechanism, the thermochemical unfeasibility of SET indicates that also SEPT is not a viable mechanism. Therefore, only three mechanisms are going to be considered henceforth: RAF, HAT, and PCET.

The RAF mechanism was found to be exergonic for the  $\cdot\text{OH}$  reactions, while it leads to positive values of  $\Delta G$  for the SAC reactions involving the HOO $^{\bullet}$  radical. This indicates that the formation of  $\cdot\text{OH}$  adducts is possible, while the formation of HOO $^{\bullet}$  adduct is not. Accordingly, the RAF mechanism has also been ruled out. Since all the carbon atoms in SPC are sp<sup>3</sup>, the RAF mechanism has not been modeled for SPC.

Since HAT and PCET yield exactly the same products, the values of  $\Delta G$  for these two processes are identical. The

**Table 2.** Gibbs Free Energies of Reaction, at 298.15 K, in kcal/mol<sup>a</sup>

	SAC		SBC		SPC
	R = $\cdot\text{OH}$	R = $\text{HOO}^{\bullet}$	R = $\cdot\text{OH}$	R = $\text{HOO}^{\bullet}$	
SET	19.75	42.80	19.83	18.85	
RAF					
site 1	-23.30	3.28	-9.76		
site 2	-21.46	4.66	-10.41		
site 2a			-8.05		
site 6			-8.95		
site 7			-10.42		
HAT/PCET					
site 1				-21.48	
site 2				-24.88	
site 3	-38.77	-5.54	-32.94	-26.50	
site 4	-24.95	8.28	-25.58	-25.18	
site 5	-25.78	7.45	-27.53	-25.12	

<sup>a</sup> SAC, S-allylcysteine; SBC, S-benzylcysteine; SPC, S-propylcysteine.

HAT/PCET mechanism was found to be largely exergonic for the  $\cdot\text{OH}$  reactions with SAC, SBC, and SPC. For the SAC + HOO $^{\bullet}$  reaction most of the channels are endergonic. The only exception is the H transfer from site 3, which was found to be exergonic by about 5.5 kcal/mol. Therefore, it seems that for this mechanism this is the only thermochemically viable channel. This channel (HAT/PCET at site 3) is therefore proposed as the one responsible for the overall HOO $^{\bullet}$  scavenging activity of SAC.

In order to identify if the corresponding transition state (TS) structures actually correspond to HAT or PCET mechanisms, three different analyses have been performed. They are based on atomic spin densities (ASD) on the sites relevant to the studied reactions, the charge ( $Q$ ) carried by the H atom that is transferred, and the electronic density of the singly occupied molecular orbital (SOMO). Based on the structural similarity of the studied compounds, these analyses have been performed only for SAC. The ASD and  $Q$  values were obtained from natural population analysis (NPA) calculations and are reported in Table 3. As the coefficients of the natural orbital carrying the unpaired electron indicate, the spin population is concentrated on the two atoms which undergo the H exchange, and a small negative value is found on the H atoms being transferred. This is consistent with a three-center three-electron bond and usually corresponds to HAT processes.<sup>54</sup> Regarding the charge carried by the H atom that is being transferred, it has been stated that migrating H's with substantial positive charge are typical of proton migrations.<sup>55,56</sup> The  $Q$  values obtained for TS3(OH), TS4(OH), TS4n(OH), TS5(OH), and TS3(HOO) are about 0.3. This value is similar to those reported for other systems undergoing HAT processes.<sup>25</sup> Therefore, the charge criterion also seems to support that these TSs correspond to the HAT mechanism.

Since it is commonly accepted that when a reaction takes place through the PCET mechanism the proton and the electron are transferred between different sets of orbitals,<sup>53</sup> the analysis of the singly occupied molecular orbital (SOMO) of the TS is also used to differentiate between HAT and PCET processes. The SOMO of HAT TSs is expected to have significant density in atomic

**Table 3.** Atomic Spin Densities (ASD) and Charge ( $Q$ ) Carried by the Migrating H Atom, from Natural Orbital Population Analyses for S-Allylcysteine (SAC) Transition States

	ASD		$Q$	
	R = $\cdot\text{OH}$	R = $\text{HOO}^{\bullet}$	R = $\cdot\text{OH}$	R = $\text{HOO}^{\bullet}$
TS3				
C3	0.205	0.315		
H	-0.042	-0.035	0.307	0.373
O	0.771	0.450		
TS4				
C4	0.215			
H	-0.039		0.279	
O	0.758			
TS4n				
C4	0.292	-		
H	-0.044	-	0.324	-
O	0.735	-		
TS5				
C5	0.317	-		
H	-0.045	-	0.339	-
O	0.713	-		

orbitals oriented along, or nearly along, the transition vector (donor---H---acceptor). The SOMOs of PCET TSs, on the other hand, involve p orbitals that are orthogonal to the donor---H---acceptor vector.<sup>53</sup> As the plots in Figure 3 show the SOMOs in all the TSs associated with hydrogen transfers, there is a node at the migrating H that is mostly localized on the C---H---O vector, which corresponds to HAT transition states. Therefore, according to all analyzed criteria, transition states TS3(OH), TS4(OH), TS5(OH), and TS3(HOO) all correspond to the HAT mechanism; i.e., none of the studied channels of reaction correspond to PCET processes.

The fully optimized structures of all the studied transition states are shown in Figures 4, 5, and 6 for SAC, SBC, and SPC, respectively. For the reactions of SAC (Figure 4), TS1(OH) and TS2(OH) correspond to RAF processes, while all the others have been identified as HAT transition states. TS1(OH) was found to be earlier than TS2(OH), suggesting that the barrier of the former should be lower than that of the latter one. No stabilizing interactions were found for either of them. The HAT transition states, on the other hand, all show hydrogen-bond-like interactions between the radical and the SAC fragments. Two conformations, significantly different in energy, were located for the H transfer from site 4, depending on the migrating H. For TS3(OH), TS4(OH), TS4n(OH), and TS5(OH) the interaction involves the H atom in the  $\cdot\text{OH}$  radical and one of the O atoms in the carboxylate group of zwitterionic SAC. The interaction distance,  $d(\text{H}\cdots\text{O})$ , was found to be 1.883, 1.788, 2.004, and 2.143 Å, respectively. For TS3(HOO) the interaction involves the H atom in the HOO $^{\bullet}$  moiety and one of the O atoms in the carboxylate group of SAC, with  $d(\text{H}\cdots\text{O})$  = 1.658 Å. These interactions are important since it has been previously reported that they lower the reaction barriers.<sup>57</sup>

For the reactions involving SBC (Figure 5), TS1(OH), TS2(OH), TS6(OH), and TS7(OH) correspond to RAF processes, while all the others are HAT transition states. Two different

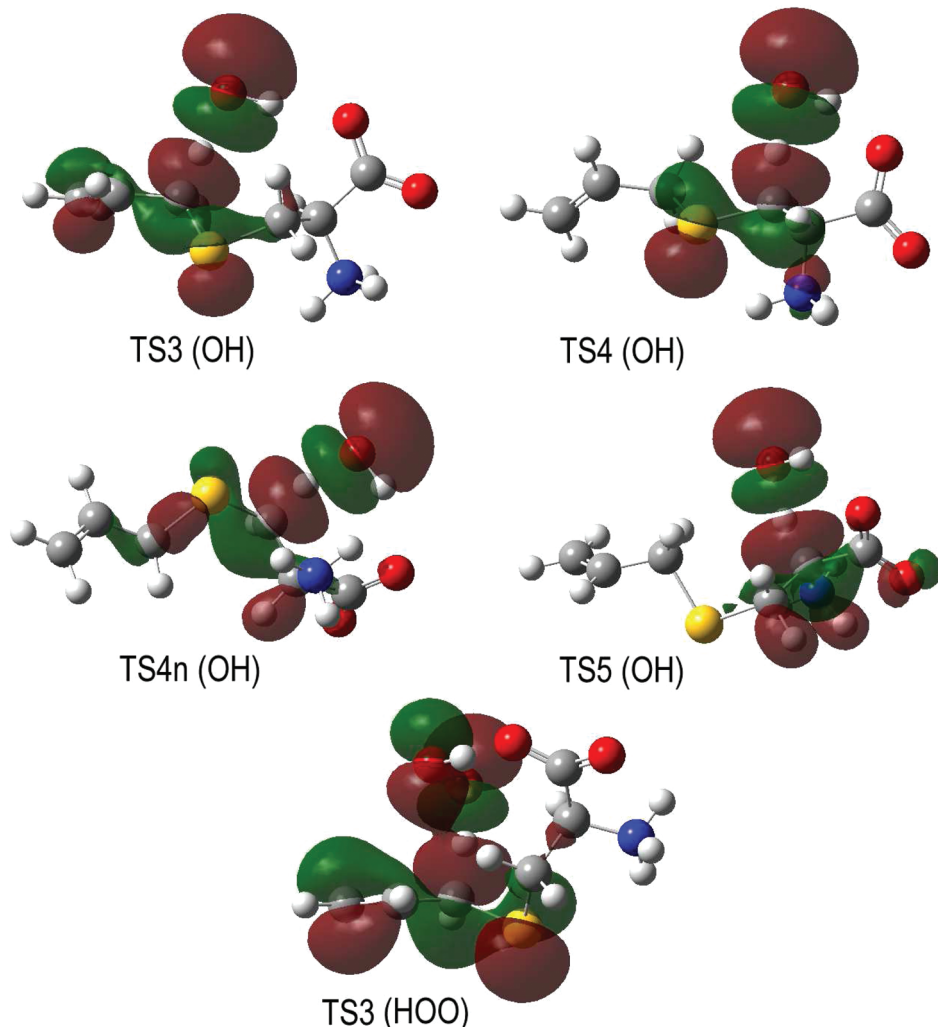


**Figure 3.** SOMO density surfaces of the HAT transition state structures involving S-allylcysteine (SAC), computed with an isodensity value of 0.02 au.

conformations have been identified for  $\cdot\text{OH}$  additions to site 2 of SBC; they are TS2a(OH) and TS2s(OH). They correspond to antiperiplanar and synclinal orientations, respectively, with respect to the sulfur atom. TS2a(OH) was found to be earlier than TS2s(OH), suggesting that the barrier of the former should be lower than that of the latter one. No stabilizing interactions were found for them, nor for the other RAF transition states. The HAT transition states, on the other hand, show hydrogen-bond-like interactions. All of them involve the H in the radical and one of the O atoms in the carboxylate group of zwitterionic SBC. The interaction distances,  $d(\text{H} \cdots \text{O})$ , were found to be 1.876, 1.789, 2.030, and 2.075 Å for TS3(OH), TS4(OH), TS4n(OH), and TS5(OH), respectively.

For the reactions involving SPC (Figure 6), all transition states correspond to the HAT mechanism, since RAF has been ruled out based on the structure of this compound. With the exception of TS1(OH) all TSs show hydrogen-bond-like interactions. In TS2(OH) this interaction involves the H in the  $\cdot\text{OH}$  and the S atom in SPC. For all the other TS structures it takes place between the H in the radical and one of the O atoms in the carboxylate group of SPC. The interaction distances are 2.658, 1.885, 1.801, 1.993, and 2.120 Å, for TS2(OH), TS3(OH), TS4(OH), TS4n(OH), and TS5(OH), respectively.

Reactant complexes (RCs) were located in the entrance channels of the HAT reactions. They are relevant to the kinetics of such reactions since there is a possibility of quantum mechanical tunneling. Since the reactions take place in solution, RCs are collisionally stabilized. Therefore all energy levels from the bottom of the well up to the top of the barrier will contribute to the tunneling. The optimized geometries of the reactant complexes are shown in Figure 7. For the SAC reaction with  $\cdot\text{OH}$ , two reactant complexes were identified: RC(OH)a and RC(OH)b. The first one connects with TS4n(OH), while the second one connects with TS3(OH), TS4(OH), and TS5(OH). All the RCs are formed by H-bond-like interactions between the H atom in the oxygenated radical and one of the O atoms in the carboxylate group in SAC. The interaction distances were found to be 1.771, 1.704, and 1.421 Å for SAC-RC(OH)a, SAC-RC(OH)b, and SAC-RC(HOO), respectively. Their relative Gibbs free energies, with respect to the isolated reactants, are 0.25, -0.19, and -3.42 kcal/mol.

For the SBC one RC was located for its reaction with  $\cdot\text{OH}$ . The H-bond-like interactions leading to the formation of the RCs involve the H atom in the oxygenated radical and one of the O atoms in the carboxylate group of SBC. The interaction distance was found to be 1.699 Å. Its relative Gibbs free energy, with

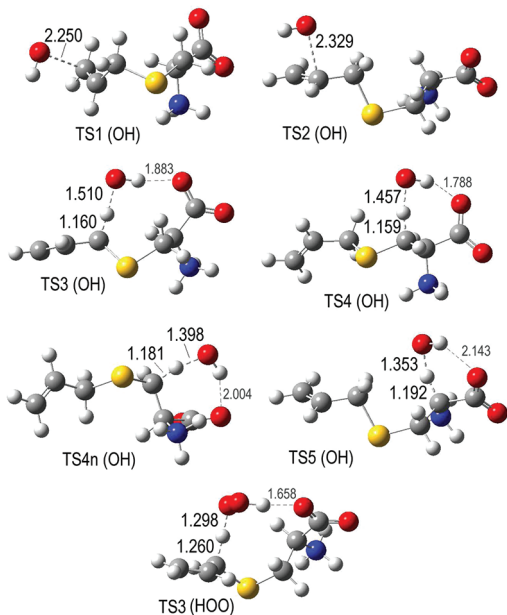


**Figure 4.** Optimized geometries of RAF and HAT transition states for S-allylcysteine (SAC) reactions with hydroxyl ( $\cdot\text{OH}$ ) and peroxy ( $\text{HOO}^\bullet$ ) radicals.

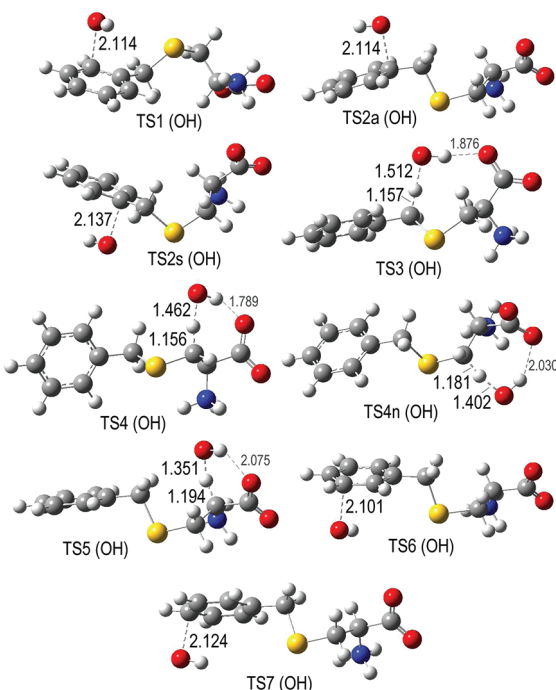


**Figure 5.** Optimized geometries of RAF and HAT transition states for S-benzylcysteine (SBC) reactions with hydroxyl radical ( $\cdot\text{OH}$ ).

respect to the isolated reactants is  $-2.02 \text{ kcal/mol}$ . For SPC also one RC was identified. The interaction distance between the H atom in the radical and one of the O atoms in the carboxylate group in SPC was found to be  $1.698$ . This RC is  $1.25 \text{ kcal/mol}$  lower in Gibbs free energy than the isolated reactants.

The barriers of reaction, in terms of Gibbs free energies, relative to the isolated reactants ( $\Delta G^\ddagger$ ), are reported in Table 4. As these values show, the lowest barriers for the SAC +  $\cdot\text{OH}$

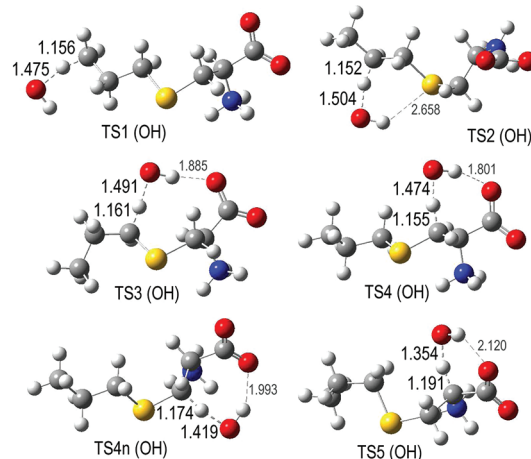


**Figure 6.** Optimized geometries of HAT transition states for S-prolylcysteine (SPC) reactions with hydroxyl radical ( $\cdot\text{OH}$ ).

reaction correspond to the RAF processes, while it corresponds to HAT from site 4 for the SBC +  $\cdot\text{OH}$  reaction. For SPC the HAT from site 4 has also the lowest barrier. The barrier for  $\cdot\text{OH}$  addition to site 1 was found to be slightly lower than that of site 2 for SAC. Both of them are significantly lower than any of the RAF barriers corresponding to the SBC reactions. For the latter the lowest RAF barrier corresponds to the  $\cdot\text{OH}$  addition to site 2, through the antiperiplanar TS. Comparing HAT processes at site 3 of SAC for the reactions involving  $\cdot\text{OH}$  and  $\text{HOO}^\bullet$ , it can be noticed that the barrier of the latter is significantly higher, which is in line with the lower reactivity of the  $\text{HOO}^\bullet$ , compared to that of the  $\cdot\text{OH}$ .

The rate constants and the branching ratios of the studied channels are reported in Table 5, together with the overall rate coefficients. For the SAC +  $\text{HOO}^\bullet$  reaction there is only one viable channel, but for the reactions of SAC, SBC, and SPC with  $\cdot\text{OH}$  there are several channels contributing to the overall reactivity of these compounds. We have assumed that neither mixing nor crossover between different pathways occurs, and therefore the overall rate coefficient has been calculated as the sum of the rate coefficients of each channel:

$$k_{\text{OH} + \text{SAC}}^{\text{overall}} = k_{\text{app}, \text{OH} + \text{SAC}}^{\text{RAF}} + k_{\text{app}, \text{OH} + \text{SAC}}^{\text{HAT}} \quad (5)$$

$$k_{\text{OH} + \text{SBC}}^{\text{overall}} = k_{\text{app}, \text{OH} + \text{SBC}}^{\text{RAF}} + k_{\text{app}, \text{OH} + \text{SBC}}^{\text{HAT}} \quad (6)$$

$$k_{\text{OH} + \text{SPC}}^{\text{overall}} = k_{\text{app}, \text{OH} + \text{SPC}}^{\text{HAT}} \quad (7)$$

where

$$k_{\text{app}, \text{OH} + \text{SAC}}^{\text{RAF}} = k_{\text{app}}^{\text{C1(SAC)}} + k_{\text{app}}^{\text{C2(SAC)}} \quad (8)$$

$$k_{\text{app}, \text{OH} + \text{SAC}}^{\text{HAT}} = k_{\text{app}}^{\text{C3(SAC)}} + k_{\text{app}}^{\text{C4(SAC)}} + k_{\text{app}}^{\text{C5(SAC)}} \quad (9)$$

$$k_{\text{app}, \text{OH} + \text{SBC}}^{\text{RAF}} = k_{\text{app}}^{\text{C1(SBC)}} + k_{\text{app}}^{\text{C2(SBC)}} + k_{\text{app}}^{\text{C6(SBC)}} + k_{\text{app}}^{\text{C7(SBC)}} \quad (10)$$

$$k_{\text{app}, \text{OH} + \text{SBC}}^{\text{HAT}} = k_{\text{app}}^{\text{C3(SBC)}} + k_{\text{app}}^{\text{C4(SBC)}} + k_{\text{app}}^{\text{C5(SBC)}} \quad (11)$$

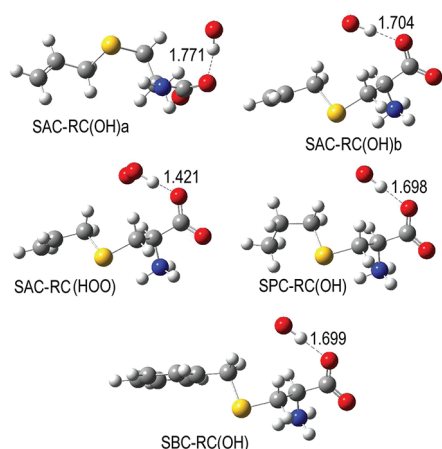


Figure 7. Optimized geometries of the reactant complexes.

Table 4. Gibbs Free Energies of Activation, at 298.15 K, in kcal/mol, Relative to Isolated Reactants<sup>a</sup>

	SAC		SBC		SPC	
	R = OH <sup>•</sup>	R = HOO <sup>•</sup>	R = OH <sup>•</sup>	R = HOO <sup>•</sup>	R = OH <sup>•</sup>	R = HOO <sup>•</sup>
<b>RAF</b>						
site 1	3.46		7.48			
site 2a	3.71		6.23			
site 2s			8.87			
site 6			6.40			
site 7			6.11			
<b>HAT</b>						
site 1				8.14		
site 2				7.04		
site 3	5.76	17.64	6.04	6.49		
site 4	6.26		5.97	4.85		
site 4n	8.55		8.16	8.81		
site 5	10.06		10.01	10.24		

<sup>a</sup> SAC, S-allylcysteine; SBC, S-benzylcysteine; SPC, S-propylcysteine.

$$k_{\text{app}, \text{OH} + \text{SPC}}^{\text{HAT}} = k_{\text{app}}^{\text{C1}(SPC)} + k_{\text{app}}^{\text{C2}(SPC)} + k_{\text{app}}^{\text{C3}(SPC)} + k_{\text{app}}^{\text{C4}(SPC)} + k_{\text{app}}^{\text{CS}(SPC)} \quad (12)$$

The branching ratios of the different reaction channels, which represent the percent of their contribution to the overall reaction, have been calculated as

$$\Gamma_i = \frac{k_{i, \text{SXC}}}{k_{\text{overall}(\text{SXC})}} \cdot 100 \quad (13)$$

where *i* represents each particular channel and SXC = SAC, SBC, or SPC.

As the values in Table 5 show, all channels of reaction significantly contribute to the overall reactivity of SAC, SBC, and SPC toward OH<sup>•</sup>, with the exception of HAT from site 5, which is predicted to contribute less than 1% for all the studied scavengers. Both mechanisms, RAF and HAT, are important for the OH<sup>•</sup> reactions with SAC and SBC. Their contributions are %HAT(SAC) = 39.6%, %RAF(SAC) = 60.4%, %HAT(SBC) =

Table 5. Apparent Rate Constants (*k*) and Branching Ratios ( $\Gamma$ ) of the Different Channels of Reaction with the Hydroxyl Radical (OH<sup>•</sup>), and Overall Rate Coefficient (M<sup>-1</sup> s<sup>-1</sup>), at 298 K<sup>a</sup>

	SAC		SBC		SPC	
	<i>k</i>	$\Gamma$	<i>k</i>	$\Gamma$	<i>k</i>	$\Gamma$
<b>RAF</b>						
site 1	$1.20 \times 10^9$	30.6	$7.18 \times 10^7$	2.8		
site 2	$1.17 \times 10^9$	29.8	$1.59 \times 10^8$	6.1		
site 6			$3.59 \times 10^8$	13.9		
site 7			$3.10 \times 10^8$	12.0		
<b>HAT</b>						
site 1					$3.41 \times 10^7$	1.6
site 2					$8.54 \times 10^7$	3.9
site 3	$1.08 \times 10^9$	27.5	$8.26 \times 10^8$	32.0	$6.55 \times 10^8$	30.0
site 4	$4.64 \times 10^8$	11.9	$8.40 \times 10^8$	32.5	$1.41 \times 10^9$	64.3
site 5	$8.96 \times 10^6$	0.2	$1.79 \times 10^7$	0.7	$5.95 \times 10^6$	0.3
overall	$3.91 \times 10^9$		$2.58 \times 10^9$		$2.19 \times 10^9$	

<sup>a</sup> SAC, S-allylcysteine; SBC, S-benzylcysteine; SPC, S-propylcysteine.

65.2%, and %RAF(SBC) = 34.8%. This means that the nature of the scavenger plays an important role in the preponderant mechanism of reaction. For SPC the OH<sup>•</sup> scavenging activity takes place exclusively through HAT. For SBC this is the main mechanism but RAF contributes to a significant proportion. For SAC, on the other hand, RAF is the main mechanism, but HAT is also significant to the overall reactivity toward OH<sup>•</sup>.

For the SAC + OH<sup>•</sup> process, both channels of the RAF mechanism similarly contribute to the overall reaction, while among the HAT channels site 3 is predicted to be significantly faster than the others. For the reaction with SBC the major contributors to the RAF mechanism are the OH<sup>•</sup> additions to the ring, in particular to sites 6 and 7. For this scavenger HAT channels from sites 3 and 4 are predicted to be the fastest channels with similar contributions to the overall reactivity. In the case of SPC, which can only react through HAT, the main channel of reaction was found to be that involving H transfer from site 4. All the overall rate coefficients, of the reactions with OH<sup>•</sup>, were found to be close to the diffusion limit. However, SAC was found to react 1.5 and 1.8 times faster than SBC and SPC, respectively. This order is in agreement with the experimental evidence.

The reaction of SAC with HOO<sup>•</sup> was found to be considerably slower than that involving OH<sup>•</sup>. The rate constant of SAC + HOO<sup>•</sup> is predicted to be  $7.53 \times 10^2 \text{ M}^{-1} \text{ s}^{-1}$ , at room temperature. Accordingly, this scavenger reacts with OH more than  $10^6$  times faster than with HOO<sup>•</sup>. Based on their structural similarities, a similar behavior is also expected for SBC and SPC.

The computational results suggests that SAC, SBC, and SPC are excellent OH<sup>•</sup> scavengers, but only moderately efficient as HOO<sup>•</sup> radical scavengers. There are previous reports on the kinetics of other compounds, present in garlic, when reacting with HOO<sup>•</sup> radicals. The rate constant of the SAC + HOO<sup>•</sup> reaction is about twice that of allicin and significantly lower than that of 2-propenesulfenic acid, a precursor and decomposition product of allicin.<sup>58</sup>

According to the branching ratios for the OH<sup>•</sup> reactions with SAC, SBC, and SPC, a wide product distribution is expected. For the HOO<sup>•</sup> reactions with SAC, on the other hand, only one

product is predicted to be formed: that corresponding to a HAT process from site 3.

## CONCLUSIONS

The experimental findings suggest that SAC is better scavenger of  $\cdot\text{OH}$  than it is of  $\text{ROO}^\bullet$  and that the existence of an allyl group attached to the sulfur atom of cysteinyl group is important for the antioxidant capacity of SAC.

The computational findings suggested that SAC, SBC, and SPC can be proposed as excellent  $\cdot\text{OH}$  scavengers, while SAC is only a modest  $\text{HOO}^\bullet$  scavenger.

The calculated overall rate coefficient of the SAC reaction with  $\cdot\text{OH}$  was found to be close to the diffusion limit, and more than  $10^6$  times larger than that involving  $\text{HOO}^\bullet$ .

SAC was found to react with  $\text{HOO}^\bullet$  twice as fast as allicin and much slower than 2-propenesulfenic acid.

A wide product distribution is expected for the  $\text{OH}^\bullet$  reactions with SAC, SBC, and SPC, while for the  $\text{HOO}^\bullet$  reactions only one product is predicted: that corresponding to a HAT process from site 3.

Finally, based on its protective effects against free radicals, SAC can be proposed as a therapeutic agent or as a dietary supplement.

## AUTHOR INFORMATION

### Corresponding Author

\*E-mail: agalano@prodigy.net.mx or agal@xanum.uam.mx (A.G.); maldonado.perla@gmail.com (P.D.M.).

## ACKNOWLEDGMENT

This work was supported by CONACYT 103527 (P.D.M.) and PAPIIT IN2019101 (J.P.-C.). A.G. thanks Laboratorio de Visualización y Cómputo Paralelo at UAM-Iztapalapa for access to its computer facilities. J.R.A.-I. thanks the Dirección General de Servicios de Cómputo Académico (DGSCA) at Universidad Nacional Autónoma de México.

## REFERENCES

- (1) Wakunaga of America Co, LTD. *Aged Garlic Extract. Research Excerpts from Peer Reviewed Scientific Journals & Scientific Meetings*; Wakunaga of America Co, LTD.: Mission Viejo, CA, 2006; pp 1–63.
- (2) Lawson, L. D. In *Phytomedicines of Europe. Chemistry and Biological Activity*; Lawson, L. D., Bauer, R., Eds.; ACS Symposium Series 691; American Chemical Society: Washington, DC, 1998; pp 176–209.
- (3) Borek, C. *J. Nutr.* **2001**, *131*, 1010S–1015S.
- (4) Koderer, Y.; Suzuki, A.; Imada, O.; Kasuga, S.; Sumioka, I.; Kanezawa, A.; Taru, N.; Fujikawa, M.; Nagae, S.; Masamoto, K.; Maeshige, K.; Ono, K. *J. Agric. Food Chem.* **2002**, *50*, 622.
- (5) Amagase, H.; Petesch, B. L.; Matsuura, H.; Kasuga, S.; Itakura, Y. *J. Nutr.* **2001**, *131*, 955S.
- (6) Kim, K. M.; Chun, S. B.; Koo, M. S.; Choi, W. J.; Kim, T. W.; Kwon, Y. G.; Chung, H. T.; Billiar, T. R.; Kim, Y. M. *Free Radical Biol. Med.* **2001**, *30*, 747.
- (7) Maldonado, P. D.; Barrera, D.; Rivero, I.; Mata, R.; Medina-Campos, O. N.; Hernandez-Pando, R.; Pedraza-Chaverri, J. *Free Radical Biol. Med.* **2003**, *35*, 31.
- (8) Medina-Campos, O. N.; Barrera, D.; Segoviano-Murillo, S.; Rocha, D.; Maldonado, P. D.; Mendoza-Patiño, N.; Pedraza-Chaverri, J. *Food Chem. Toxicol.* **2007**, *45*, 2030.
- (9) Ide, N.; Lau, B. H. *J. Nutr.* **2001**, *131*, 1020S.
- (10) Ide, N.; Lau, B. H. *Drug Dev. Ind. Pharm.* **1999**, *25*, 619.
- (11) Ho, S. E.; Ide, N.; Lau, B. H. *Phytomedicine* **2001**, *8*, 39.
- (12) Chung, L. Y. *J. Med. Food* **2006**, *9*, 205.
- (13) Numagami, Y.; Ohnishi, S. T. *J. Nutr.* **2001**, *131*, 1100S.
- (14) Kim, J. M.; Lee, J. C.; Chang, N.; Chun, H. S.; Kim, W. K. *Free Radical Res.* **2006**, *40*, 827.
- (15) Yamasaki, T.; Lau, B. H. *Nihon Yakurigaku Zasshi* **1997**, *110*, 138P.
- (16) Ide, N.; Lau, B. H. *J. Pharm. Pharmacol.* **1997**, *49*, 908.
- (17) Imai, J.; Ide, N.; Nagae, S.; Moriguchi, T.; Matsuura, H.; Itakura, Y. *Planta Med.* **1994**, *60*, 417.
- (18) Numagami, Y.; Sato, S.; Ohnishi, S. T. *Neurochem. Int.* **1996**, *29*, 135.
- (19) Moriguchi, T.; Matsuura, H.; Koderer, Y.; Itakura, Y.; Katsuki, H.; Saito, H.; Nishiyama, N. *Neurochem. Res.* **1997**, *22*, 1449.
- (20) Nishiyama, N.; Moriguchi, T.; Morihara, N.; Saito, H. *J. Nutr.* **2000**, *131*, 1093S.
- (21) Kim, J. M.; Chang, H. J.; Kim, W. K.; Chang, N.; Chun, H. S. *J. Agric. Food Chem.* **2006**, *54*, 6547.
- (22) Lissi, E.; Salim-Hanna, M.; Pascual, C.; del Castillo, M. D. *Free Radical Biol. Med.* **1995**, *18*, 153.
- (23) Kocha, T.; Yamaguchi, M.; Ohtaki, H.; Fukuda, T.; Aoyagi, T. *Biochim. Biophys. Acta* **1997**, *1337*, 319.
- (24) Zhao, Y.; Schultz, N. E.; Truhlar, D. G. *J. Chem. Theory Comput.* **2006**, *2*, 364.
- (25) Zavala-Oseguera, C.; Alvarez-Idaboy, J. R.; Merino, G.; Galano, A. *J. Phys. Chem. A* **2009**, *113*, 13913.
- (26) Velez, E.; Quijano, J.; Notario, R.; Pabón, E.; Murillo, J.; Leal, J.; Zapata, E.; Alarcón, G. *J. Phys. Org. Chem.* **2009**, *22*, 971.
- (27) Vega-Rodriguez, A.; Alvarez-Idaboy, J. R. *Phys. Chem. Chem. Phys.* **2009**, *11*, 7649.
- (28) Galano, A.; Alvarez-Idaboy, J. R. *Org. Lett.* **2009**, *11*, 5114.
- (29) Black, G.; Simmie, J. M. *J. Comput. Chem.* **2010**, *31*, 1236.
- (30) Furuncuoglu, T.; Ugur, I.; Degirmenci, I.; Aviyente, V. *Macromolecules* **2010**, *43*, 1823.
- (31) Galano, A.; Macías-Ruvalcaba, N. A.; Campos, O. N. M.; Pedraza-Chaverri, J. *J. Phys. Chem. B* **2010**, *114*, 6625.
- (32) Young, D. *Computational Chemistry: A Practical Guide for Applying Techniques to Real World Problems*; John Wiley & Sons: New York, 2001; pp 227–228.
- (33) Allodi, M. A.; Kirschner, K. N.; Shields, G. C. *J. Phys. Chem. A* **2008**, *112*, 7064.
- (34) Frisch, M. J.; Trucks, G. W.; Schlegel, H. B.; Scuseria, G. E.; Robb, M. A.; Cheeseman, J. R.; Scalmani, G.; Barone, V.; Mennucci, B.; Petersson, G. A.; et al. *Gaussian 09*, revision A.08; Gaussian, Inc.: Wallingford, CT, 2009.
- (35) Marenich, A. V.; Cramer, C. J.; Truhlar, D. G. *J. Phys. Chem. B* **2009**, *113*, 6378.
- (36) Okuno, Y. *Chem.—Eur. J.* **1997**, *3*, 210.
- (37) Benson, S. W. *The Foundations of Chemical Kinetics*; Krieger: Malabar, FL, 1982; Chapter XV.
- (38) Ardura, D.; Lopez, R.; Sordo, T. L. *J. Phys. Chem. B* **2005**, *109*, 23618.
- (39) Alvarez-Idaboy, J. R.; Reyes, L.; Cruz, J. *Org. Lett.* **2006**, *8*, 1763.
- (40) Alvarez-Idaboy, J. R.; Reyes, L.; Mora-Diez, N. *Org. Biomol. Chem.* **2007**, *5*, 3682.
- (41) Galano, A. *J. Phys. Chem. A* **2007**, *111*, 1677.
- (42) Galano, A. *J. Phys. Chem. C* **2008**, *112*, 8922.
- (43) Galano, A.; Cruz-Torres, A. *Org. Biomol. Chem.* **2008**, *6*, 732.
- (44) Galano, A.; Francisco-Márquez, M. *Chem. Phys.* **2008**, *345*, 87.
- (45) Mora-Diez, N.; Keller, S.; Alvarez-Idaboy, J. R. *Org. Biomol. Chem.* **2009**, *7*, 3682.
- (46) Eyring, H. *J. Chem. Phys.* **1935**, *3*, 107.
- (47) Evans, M. G.; Polanyi, M. *Trans. Faraday Soc.* **1935**, *31*, 875.
- (48) Truhlar, D. G.; Hase, W. L.; Hynes, J. T. *J. Phys. Chem.* **1983**, *87*, 2664.
- (49) Eckart, C. *Phys. Rev.* **1930**, *35*, 1303.
- (50) Collins, F. C.; Kimball, G. E. *J. Colloid Sci.* **1949**, *4*, 425.
- (51) Smoluchowski, M. *Z. Phys. Chem.* **1917**, *92*, 129.

- (52) Truhlar, D. G. *J. Chem. Educ.* **1985**, *62*, 104.
- (53) (a) Einstein, A. *Ann. Phys. (Leipzig)* **1905**, *17*, 549.(b) Stokes, G. G. *Mathematical and Physical Papers*; Cambridge University Press: Cambridge, U.K., 1903; Vol. 3, p 55.
- (54) Olivella, S.; Anglada, J. M.; Solý, A.; Bofill, J. M. *Chem.—Eur. J.* **2004**, *10*, 3404.
- (55) Mayer, J. M.; Hrovat, D. A.; Thomas, J. L.; Borden, W. T. *J. Am. Chem. Soc.* **2002**, *124*, 11142.
- (56) Turecek, F.; Syrstad, E. A. *J. Am. Chem. Soc.* **2003**, *125*, 3353.
- (57) See, for example: (a) Galano, A.; Alvarez-Idaboy, J. R.; Bravo-Perez, G.; Ruiz-Santoyo, M. E. *J. Mol. Struct.: THEOCHEM* **2002**, *617*, 77–86. (b) Uc, V. H.; Alvarez-Idaboy, J. R.; Galano, A.; Garcia-Cruz, I.; Vivier-Bunge, A. *J. Phys. Chem. A* **2006**, *110*, 10155–10162. (c) Galano, A.; Alvarez-Idaboy, J. R. Chapter 12 Atmospheric Reactions of Oxygenated Volatile Organic Compounds + OH Radicals: Role of Hydrogen-Bonded Intermediates and Transition States. *Adv. Quantum Chem.* **2008**, *55*, 245–274. (d) Galano, A.; Cruz-Torres, A. *Org. Biomol. Chem.* **2008**, *6*, 732.
- (58) Galano, A.; Francisco-Márquez, M. *J. Phys. Chem. B* **2009**, *113*, 16077.